

Multiresonant Nanolaminate Nanopillar Arrays for Broadband Nonlinear Optics and Enhanced Refractive Index Sensing

Meitong Nie¹, Yuming Zhao¹, Aditya Garg¹, Elieser Mejia¹, Chuan Xiao¹, Junyeob Song², Benjamin Pittelkau¹, Seied Ali Safiabadi Tali¹, Linbo Shao^{1,3}, and Wei Zhou^{1,*}

¹Bradley Department of Electrical & Computer Engineering, Virginia Tech, Blacksburg, Virginia 24061, USA.

²Physical Measurement Laboratory, National Institute of Standards and Technology, Gaithersburg, Maryland 20899, USA

³Center for Quantum Information Science and Engineering (VTQ), Virginia Tech, Blacksburg, Virginia 24061, USA

*Corresponding author: wzh@vt.edu

Abstract: Multiresonant nanolaminate nanopillar arrays (NLNPAs) enable broadband second- and third-harmonic generation and enhanced refractive index sensing with superior sensitivity, establishing NLNPAs as a versatile platform for advanced photonic applications.

1. Introduction

Plasmonics has advanced modern optics by enabling subwavelength confinement and enhancement of electromagnetic fields through surface plasmon resonances, driving applications in sensing, imaging, and photonic circuits [1]. Combined with nonlinear optics, it enhances processes like second- and third-harmonic generation (SHG and THG), crucial for frequency conversion, photonic devices, and biological sensing [2, 3]. However, traditional plasmonic designs are narrowband, limiting their utility in broadband applications. While multiresonant systems address this, challenges persist in achieving broad operational ranges, efficient mode overlap, compact footprints, and seamless integration with functional and biological platforms [4]. To overcome these limitations, there is a need for plasmonic substrates capable of broadband, spatially overlapped multiresonant enhancement within a compact architecture. This study presents nanolaminate nanopillar arrays (NLNPAs) as a solution, demonstrating their potential for broadband nonlinear optical applications and enhanced refractive index sensing, particularly in biologically relevant environments.

2. Results and discussion

NLNPAs were fabricated by depositing metal-insulator-metal (MIM) thin films onto pre-patterned nanopillar arrays via physical vapor deposition (Fig. 1A). SEM images (Fig. 1B) reveal a periodic nanopillar structure with a diameter of 220 nm, height of 90 nm, and alternating MIM layers consisting of gold (10 nm, 10 nm, and 20 nm from bottom to top) and SiO₂ (10 nm and 15 nm from bottom to top). The measured absorption spectrum (Fig. 1C) demonstrates strong, broad absorption spanning the visible to near-infrared regions. Nonlinear optical performance was assessed by measuring nonlinear emission intensity as a function of excitation wavelength (1000–1500 nm) (Fig. 1D). The NLNPAs supports broadband SHG and THG, enabling efficient and broadband nonlinear emission from a single structure. Enhancement factors (EF) were evaluated by comparing the NLNPAs to a 40 nm-thick gold film with equivalent total gold thickness (Fig. 1E inset). SHG EFs ranged from 0.65×10^4 to 4.20×10^4 under 1000 to 1500 nm excitations, while THG EFs ranged from 0.55×10^5 to 2.02×10^5 under 1300 to 1500 nm excitations shown in Fig. 1E. These results demonstrate the NLNPAs can effectively amplify both SHG and THG over a broadband, establishing it as a promising platform for broadband nonlinear optical applications.

We further compared the linear and nonlinear signal based refractive index (RI) sensing ability based on NLNPAs. We measured reflection spectra in environments with varying RIs (1.0, 1.35, 1.40, 1.45), covering the RIs of air and biological cells (Fig. 2A). Reflection dips were broad and shallow, and the most sensitive dip yielded an RI sensitivity of 278.68 nm/RIU, lower than typical single-resonant plasmonic systems. In NLNPAs, multiple modes arise due to mode hybridization. However, geometric variation and metal losses from surface roughness broaden these resonant peaks, often causing them to merge and diminishing their quality factors. Furthermore, the differing origins of these modes may result in opposing spectral shifts upon RI changes, yielding minimal overall spectral variation. Consequently, achieving sensitive RI sensing using the linear optical response of multiresonant plasmonic NLNPAs is challenging. Then, we investigated the potential of nonlinear harmonic signals for RI sensing. Fig. 2B illustrates the dependence of nonlinear emission on the surrounding medium's RI under 1500 nm excitation. Both SHG and THG intensities rise significantly with rising RI (Fig. 2C). To further understand these trends, we performed FDTD simulations in different RI environments, with absorption spectra shown in Fig. 2D. Resonant modes are highly sensitive to the surrounding dielectric environment. As the RI increases, the absorption peak near 1500 nm redshifts toward the excitation wavelength, enhancing local electric fields at excitation wavelength. This enhancement in the

electrical fields drives the nonlinear polarization, scaling quadratically for SHG and cubically for THG, thereby amplifying their intensities. At the SHG emission wavelength, two nearby resonant modes redshift, one closer to and the other farther from the SHG wavelength, creating a complex enhancement pattern not easily predicted without detailed modeling. For THG, reduced enhancement is observed as the absorption peak near 500 nm shifts away from the THG wavelength. The simulated absorption spectra strongly align with experimental observations, underscoring the potential of nonlinear emission signals for highly sensitive RI sensing.

In summary, we demonstrated the potential of NLNPAs for broadband nonlinear optics and nonlinear-based RI sensing. The NLNPAs structure enables efficient SHG and THG with significant enhancement factors, while nonlinear harmonic signals showed high sensitivity to RI changes, supported by Finite-difference time-domain (FDTD) simulations. These findings establish NLNPAs as a versatile platform for advanced photonic applications, particularly in broadband nonlinear optics and enhanced RI sensing.

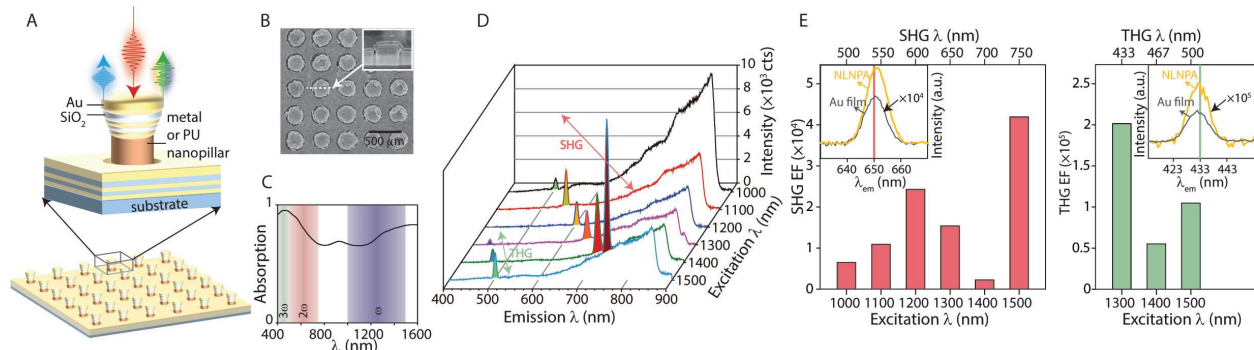


Figure 1. (A) Schematic representation of nanolaminate nanopillar arrays (NLNPAs). (B) Top-view SEM image of the NLNPAs. *Inset:* Cross-sectional SEM image of a single nanolaminate nanopillar. (C) Absorption spectrum of the NLNPAs. (D) Nonlinear emission spectra under excitations ranging from 1000 nm to 1500 nm, highlighting SHG and THG. (E) Calculated enhancement of SHG and THG compared with a 40 nm-thick gold film across various excitation wavelengths. *Inset:* Representative SHG and THG spectra from NLNPAs compared with 40 nm-thick gold film under 1300 nm excitation.

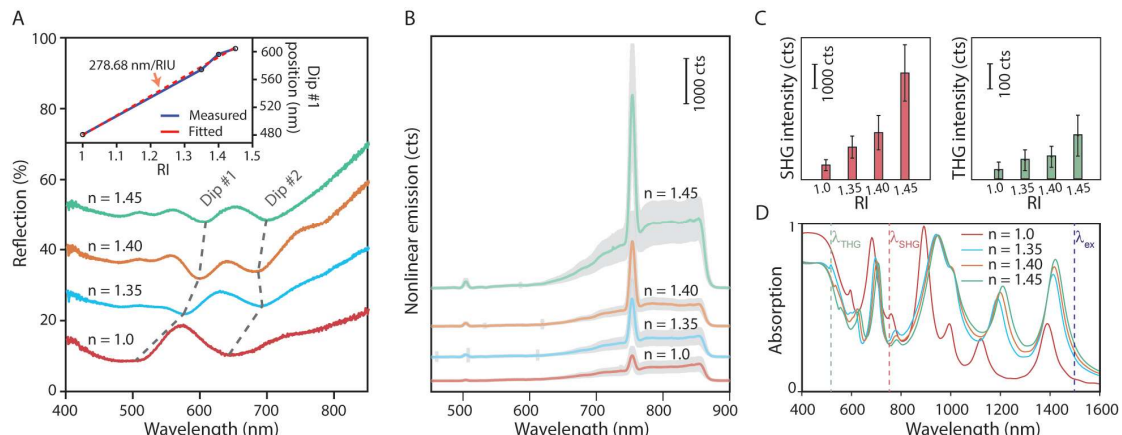


Figure 2. (A) Reflection spectra of NLNPAs in various surroundings RIs. *Inset:* position of reflection dip #1 as a function of RI. (B) Nonlinear emission spectra of NLNPAs under 1500 nm excitation for different surroundings RIs. (C) Variation of SHG and THG intensities with different surroundings RIs. (D) FDTD-simulated absorption spectra of NLNPAs in various surrounding RIs.

3. References

- [1] J.A. Schuller, E.S. Barnard, W. Cai, Y.C. Jun, J.S. White, and M.L. Brongersma, "Plasmonics for extreme light concentration and manipulation," *Nat. Mater.* **9**, 193-204 (2010).
- [2] M. Celebrano, X. Wu, M. Baselli, S. Großmann, P. Biagioni, A. Locatelli, C. De Angelis, G. Cerullo, R. Osellame, B. Hecht, and L. Duò, "Mode matching in multiresonant plasmonic nanoantennas for enhanced second harmonic generation," *Nat. Nanotechnol.* **10**, 412-417 (2015).
- [3] H. Aouani, M. Rahmani, M. Navarro-Cia, and S.A. Maier, "Third-harmonic-upconversion enhancement from a single semiconductor nanoparticle coupled to a plasmonic antenna," *Nat. Nanotechnol.* **9**, 290-294 (2014).
- [4] S.A. Safiabadi Tali, and W. Zhou, "Multiresonant plasmonics with spatial mode overlap: overview and outlook," *Nanophotonics* **8**, 1199-1225 (2019).